Microwave assisted hydrothermal synthesis and capacitive properties of RuO_2/reduced graphene oxide composites

Milica Košević, Denis Sačer*, Aleksandar Dekanski, Vladimir Panić

Institute of Chemistry, Technology and Metallurgy, Department of Electrochemistry, University of Belgrade, Njegoševa 12, Belgrade, Serbia
**Faculty of Chemical Engineering and Technology, University of Zagreb, Marulićev trg 19, Zagreb, Croatia*

Abstract

Supercapacitive RuO_2/reduced graphene oxide composites were synthesized by hydrothermal microwave-assisted single-step method at different temperatures. Syntheses were accomplished by simultaneous oxidation of Ru from $RuCl_3$ and reduction of graphene oxide in solution of various pH. Capacitive responses of obtained samples were analyzed using combined electrochemical and quartz crystal nanobalance techniques. The cyclic voltammetry and electrochemical impedance spectroscopy have been performed in H_2SO_4 and Na_2SO_4 solutions. The analysis of obtained results showed that synthesized composites are of acceptable capacitive properties. The capacitive properties of composite synthesized at neutral pH showed weakly depandance on synthesis temperature, with moderate increase of the capaticance with increasing temperature. On the other hand, composite synthesized in alkaline conditions had the higest capacitive properties at average temperature in the examined range of temperatures.

Introduction

Supercapacitors are devices capable of storing and releasing very high amounts of charge which, with good chemical and mechanical stability, offer new opportunity to satisfy specific energy demands. Nowadays, the focus of investigation is onto various materials such as metal oxides or hydroxides (MnO_2 1,2], SnO_2 [3], RuO_2 [4,5,6], IrO_2 [7], Ni oxides [8,9,10]), conductive polymers (PANI, PEDOT, PPy) [11,12] or carbon materials (graphene, carbon foam) [13,14], which were proven to have the promising capacitive or pseudocapacitive properties suitable for supercapacitors electrodesCapacitive properties of graphene can be improved by combinig graphene with transition metal oxide. Namely, graphene has tendency to agglomeration, which decreases its overall electroactive surface and thus electrochemical properties. This impairment of graphene can be overcome by synergistic effect between graphene and transition metal oxide. In this system, graphene serves as a conducting network [13] that supports redox reaction of a transtion metal oxide and enables better disperison of metal oxide as well. The aim of this work was to synthesize *in situ* reduced graphene oxide (rGO)-supported RuO_2 composites from graphene oxide and Ru^{3+}, and to examine the influence of synthesis conditions on the capacitive properties of a composite. $RuO_2{\cdot}xH_2O$ is one of the best candidates with extremely high achievable capacitance of 1580 F/g as published by Hu *et al*. [15]. Extremely high specific capacitances of $RuO_2{\cdot}xH_2O$ were achieved when small quantities of the oxide have been mixed with materials of high electronic conductivity. In such cases, high utilization of $RuO_2{\cdot}xH_2O$ was result of good proton diffusion along with good electron conductivity. As a result, microwave-assisted hydrothermal synthesis of RuO_2/rGO can lead to better electrochemical performance, mechanical stability, good control of particle size distribution and morphology of obtained materials.

Experimental

RuO_2/reduced graphene oxide (RuO_2/rGO) synthesis

RuO_2/rGO composites were synthesized at different pH and different temperatures by a simple hydrothermal microwave (MW)-assisted single-step method, starting from aqueous $RuCl_3$ solution mixed with graphene oxide aqueous solution prepared by Hummers method [16]. pH was adjusted by adding few drops of NaOH solution into the reaction mixture. The reaction mixture (6 mL) was continuously stirred at 600 rpm inside a closed reactor (10 mL) and MW irradiated isothermally to 120, 160 and 200 °C in an MW oven (Monowave 300, Anton Paar, Ashland, VA, USA). The temperature was maintained for 5 min. Afterwards the reaction mixture was cooled spontaneously to ambient temperature. The obtained composites, denoted as c-7-120, c-7-180, c-7-200, were synthesized at pH 7 at 120, 160 and 200°C, whereas c-10-120, c-10-160, c-10-200 were synthesized at pH 10 at mentioned temperatures. After MW irradiation treatment, initially brown precursor mixture of GO and $RuCl_3$ turned black suggesting successful reduction of GO and oxidation of $RuCl_3$ to RuO_2.Upon keeping, the mixture separated into colorless supernatant solution and visible sponge-like agglomerates of RuO_2/rGO composite.

Electrochemical measurements

Electrode preparation

The Pt EQCM electrode (1.22 cm^2) was washed with ethanol, acetone and bi-distilled water and afterwards electrochemically cycled in 0.1 M $HClO_4$ in potential range from -200 – 1300 mV (vs. SCE) at 100 mV s^{-1} until

a stable CV scan was achieved. Aqueous homogenous suspensions of obtained composites were applied onto Pt EQCM electrode by drop casting and allowed to dry at room temperature to form Pt/RuO_2/rGO electrodes. Electrodes were tested by cyclic voltammetry in 1 M H_2SO_4 and 0.5 M Na_2SO_4 from -100 – 1000 mV at scan rate of 50 mV s^{-1}. The usual three-electrode setup was used with EQCM Pt electrode as working electrode, Pt foil (1 cm^2) as counter electrode and saturated calomel electrode (SCE) as the reference electrode. Potentiostat used for analysis was EG&G Princeton Applied Research, model 263A, and for EIS measurements phase sensitive detector EG&G Princeton Applied Research, model 5210, at DC potential that corresponds to open circle potential of 370 mV *vs*. SCE, with the amplitude of 5 mV of sinusoidal potential in the frequency range from 100 kHz to 10 mHz, was used. For the EQCM measurements, the frequency of the quartz crystal coated with Pt was monitored by a Stanford Research System QCM 200 quartz crystal micro-balance connected to the potentiostat. The fundamental frequency was 5 MHz and the integral sensitivity was 4.85×10^{-7} Hz cm^2 g^{-1}. The area of the working electrode was 1.22 cm^2 and piezoelectrically active area was 0.427 cm^2.

Results and discussion

Cyclic voltammetry (CV)

Cyclic voltammograms of different composites synthesized at pH 7 and 10, and at different temperatures, are shown in Fig. 1. The CV responses indicate that, for composites synthesized at neutral pH, temperature increase gives rise to the registered currents. Broad and well pronounced redox peaks around 0.5 V are commonly observed in CV for hydrous $RuO_2{\cdot}xH_2O$ [17] due to reversible redox process accompanied with sorption of hydrated protons according the equation:

$$RuO_x(OH)_y + ze^- + zH^+ \Leftrightarrow RuO_{x-z}(OH)_{y+z} \quad (1)$$

Different trend was registered for composites synthesized in alkaline solution (pH 10), for which significant current rise was registered for sample c-10-160 synthesized at 160°C probably due to optimal reduction degree of graphene oxide in combination with beneficial crystallinity and water content for RuO_2 which ensure higher transport rate for protons and electrons. The obtained layer showed best capacitive properties and it was tested in both 1M H_2SO_4 and 0.5 M Na_2SO_4 solutions with simultaneous quartz crystal resonant frequency change (Fig. 2). Obtained capaciance in H2SO4 at 50 mV/s was 100 F/g.

Significant difference during polarization of a c-10-160 layer was evident in different electrolytes, accompanied with lower currents and diminishing current peaks in 0.5M Na_2SO_4 in comparison to the CV registered in 1M H_2SO_4. During anodic polarization in acidic electrolyte, frequency decreases with potential up to 360 mV suggesting incorporation of H_3O^+ into metal oxide lattice (Fig. 2b). Afterwards, frequency increases suggesting ejection of H_3O^+ at the potentials up to 1000 mV. During cathodic polarization, continuous mass gain was obtained down to 0 mV *vs*. SCE. The obtained result indicates mass change similar to the one obtained in previous investigations that are in accordance with redox reaction (1).

The impedance data of RuO_2/rGO (c-10-160) registered in 1 M H_2SO_4 at open circuit potential (370 mV) are presented in *Figure 3*. The dependences in all types of presented EIS plots indicate the transmission line response with finely distributed relaxation times [18] as follows.

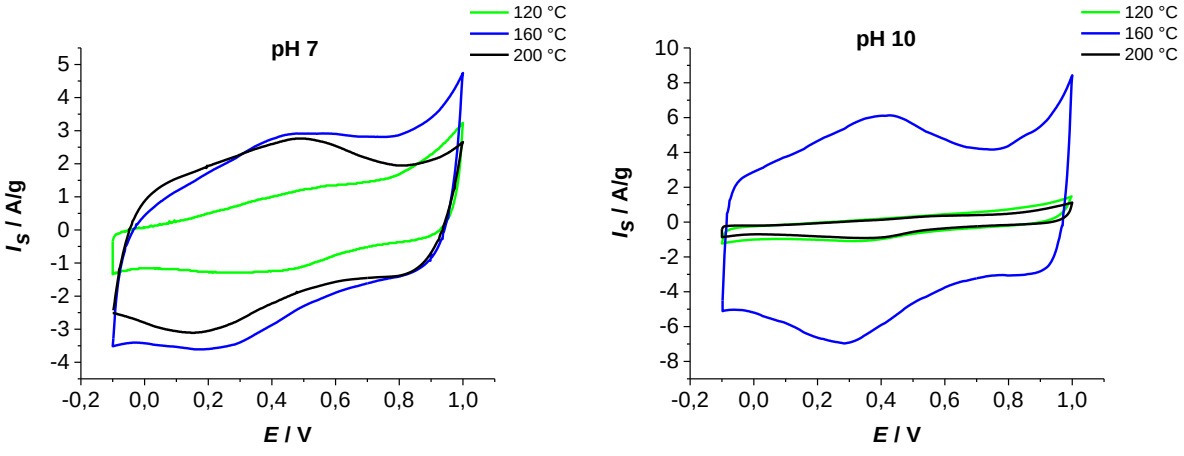

Figure 1. *Cyclic voltammograms of different composites synthesized at: a) pH 7 and b) pH 10 in 1M H_2SO_4 at scan rate 50 mV/s*

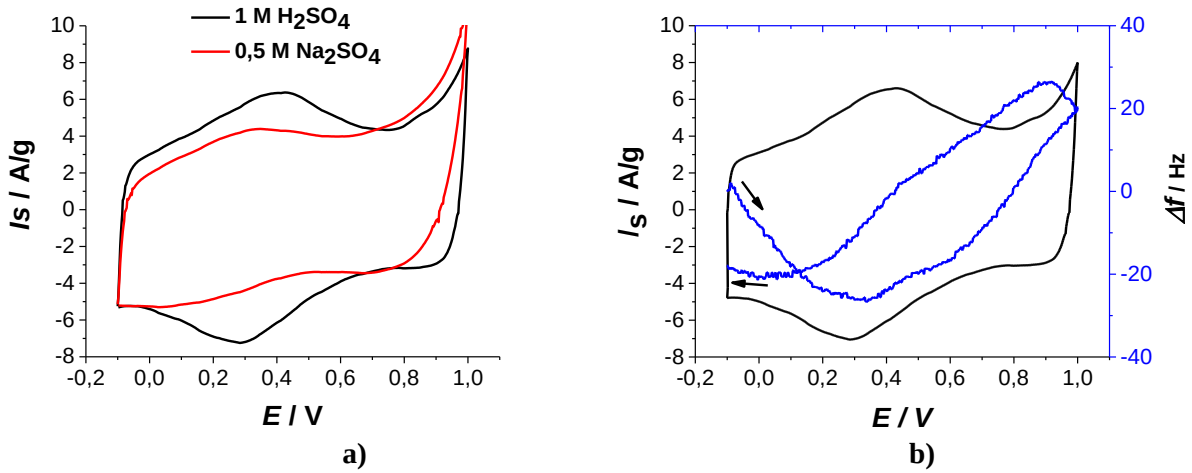

Figure 2. *Cyclic voltammograms of composite synthesized at pH 10, 160 °C in a) 1M H_2SO_4 and 0.5 M Na_2SO_4, b) in 1M H_2SO_4 with with corresponding EQCM frequency change at scan rate 50 mV/s*

The double declined linear dependence of capacitive-like response is seen in complex plane plot (*Figure 3a*) with the knee frequency positioned at quite low value (500 mHz). The declination at high frequencies (above 500 mHz) corresponds to theoretical value of 1 (0.96 is obtained with r^2 accuracy of 0.992). At frequencies below 500 mHz, typical capacitive-like response of a straight line at constant real impedance is distorted and considerably declined toward real axis. Well-resolved capacitance loops can also be hardly observed in capacitance complex plane plot (*Figure 3b*), with real capacitance ($Y_r\omega^{-1}$) not approaching $Y_i\omega^{-1}$ axis at lowest frequencies (down to 10 mHz), but a constant value between 25 and 30 mS rad^{-1} s. Bode plots (*Figure 3c*) also indicate that capacitive-like response is not reached down to 10 mHz.

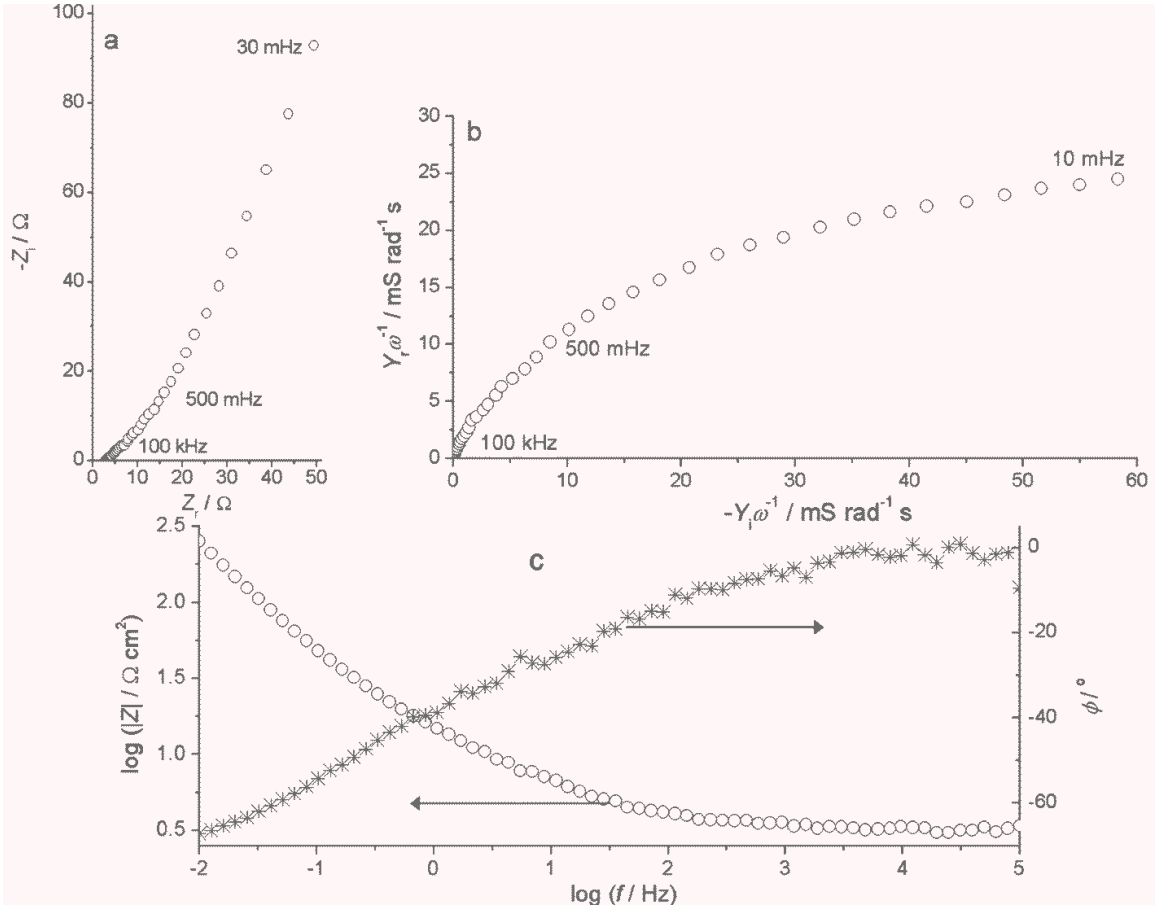

Figure 3. *The impedance and capacitance complex plane (a and b) and Bode (c) plots for the RuO_2/rGO registered in 1 M H_2SO_4 at open circuit potential.*

Constant phase shift close to –90° is not reached, while the log|*Z*|–log*f* slope below 100 mHz is –0.7 (r^2 = 0.9994), and reflects much the response related to diffusion limitations (–0.5 slope) than the capacitive-related one (the

slope of –1). All of these findings indicate that capacitive response relates to highly distributed RCs originating from the intrinsic material morphology of hardly accessible responding surfaces and/or their pronounced inhomogeneity and fractal dimensionality [19]. This morphology can be recognized as unique for rGO-based composites because of defined rGO structure of exfoliated graphite planes available for decoration by active component, *e.g.*, RuO_2, during simultaneous GO reduction/Ru oxidation as in the case of SnO_2/rGO [20]. Registered highly-pronounced transmission line response differs considerably from the responses of carbon black-supported RuO_2 [21] and RuO_2 itself [22]. This suggests that considerable amount of hardly accessible RuO_2 in RuO_2/rGO could originate from tightly stacked finely decorated rGO planes.
The difficult accessibility of loose surfaces of synthesized RuO_2/rGO composite is indicated also by the appearance to diffusion limitations-related features of Bode plots (*Figure 3c*). Besides distorted capacitive-related phase shift and modulus dependences at lowest frequencies related to transmission line distribution, ϕ–log*f* and log|*Z*|–log*f* reaches the features typical for EIS of diffusion-controlled processes at in 0.1–1 Hz frequency range. In addition, the shape of complex plate plot (*Figure 3a*) and the position of a knee frequency indicate the capacitive response accompanied by finite diffusion with reflective mass transport boundary conditions [23]. Related psudocapacitive processes apparently require considerable mass to be exchanged as found by EQCM measurements (*Figure 2b*). The largest mass gain/loss is registered around open circuit potential, which also corresponds to the position of redox processes in cyclic voltammetry response (*Figures 1 and 2*). The diffusion model with reflective mass transport boundary conditions announces the Nerst diffusion thickness much larger than that usual for finite diffusion through porous materials, which is indicated by the position of a knee frequency at quite low frequencies (*Figure 3a*). This could suggest that electrolyte species participating in redox transition processes should diffuse through the narrow gaps between tightly stacked, quite long, rGO planes decorated by RuO_2 in order to reach the most hidden inner surfaces of RuO_2/rGO. This model supposes that diffusion layer thickness should then be of the order of rGO plane length, which can explain the observed EIS features related to finite diffusion with reflective mass transport boundary conditions.

Hidrotermalna sinteza RuO_2-redukovani grafen oksid kompozita u mikrotalasnom reaktoru i njihova kapacitivna svojstva

Milica G. Košević, Denis G. Sačer*, Aleksandar Dekanski, Vladimir V. Panić

Institut za hemiju, tehnologiju i metalurgiju, Centar za elektrohemiju, Univerzitet u Beogradu, Njegoševa 12, Beograd, Srbija,
**Faculty of Chemical Engineering and Technology, University of Zagreb, Marulićev trg 19, Zagreb, Croatia*

Superkapacitivni RuO_2-redukovani grafen oksid kompoziti dobijeni su hidrotermalnom sintezom u mikrotalasnom reaktoru. Jednostepena istovremena oksidacija hidratisanog Ru^{3+} do oksida i redukcija oksida grafena izvedena jena različitim temperaturama i pH vrednostima. Kapacitivna svojstva kompozita ispitivana su cikličnom voltametrijom na elektrohemijskoj kvarc-kristalnoj nanovagi i spektroskopijom elektrohemijske impedancije u rastvorima H_2SO_4 i Na_2SO_4. Analiza dobijenih rezultata pokazuje zadovoljavajuća kapacitivna svojstva sintetisanih kompozita. Uzorak sintetisan u neutralnoj sredini pokazuje blag rast kapacitivnosti sa rastom temperature sinteze, dok je za uzorak sintetisan u baznoj kiselini najveća kapacitivnost zabeležena pri srednjoj temperaturi sinteze u primenjenom temperaturnom režimu.

References

1. X. Hu, S. Zhu, H. Huang, J. Zhang,Y. Xu, *Journal of Crystal Growth*, **434** (2016) 7
2. H. Z. Chi, S. Yin, H. Qin, K. Su , *Materials Letters*, **162** (2016) 131
3. C. Hsieh, W. Lee, C. Lee, H.Teng, *J. Phys. Chem. C*, **118** (2014) 15146
4. S. Yan, H. Wang, P. Qu, Y. Zhang, Z. Xiao, *Synthetic Metals*, **159** (2009) 158
5. S. Sopčić, M. Kraljić Roković, Z. Mandić, A. Rókab, G. Inzelt, *Electrochimica Acta*, **56** (2011) 3543
6. W. Sugimoto, T. Kizaki, K. Yokoshima, Y. Murakami, Y. Takasu, *Electrochimica Acta* **49** (2004) 313
7. D.-Q. Liu, S.-H. Yu, S.-W. Son, S.-K. Joo, *ECS Transactions*, **16** (2008) 103
8. L. Dong, Y. Chu,W. Sun, *Chem. Eur. J.*, **14** (2008) 5064
9. J. Lang, L. Kong, W. Wu, Y. Luo, L. Kang, *Chem. Commun*., (2008) 4213
10. S. Xiong, C. Yuan, X. Zhang, Y. Qian, *CrystEngComm*, **13** (2011) 626
11. H. Wang, J. Linc, Z. X. Shen, *Journal of Science: Advanced Materials and Devices*, **1** (2016) 225
12. K.Gopalakrishnan, S.Sultan, A.Govindaraj, C.N.R.Rao, *Nano Energy*, **12 (**2015) 52
13. Q. Ke, J. Wang, *J Materiomics*, **2** (2016) 37
14. Y. Shao, J. Wang, M. Engelhard, C. Wang, Y. Lin, *J. Mater. Chem.*, **20** (2010) 743

15. C.C. Hu, W. C. Chen, *Electrochim. Acta*, **49** (2004) 3469
16. H. L. Poh, F. Šaněk, A. Ambrosi, G. Zhao, Z. Sofer, M. Pumera, *Nanoscale* **4** (2012) 3515
17. S. Sopčić, Z. Mandić, G. Inzelt, M. Kraljić Roković, E. Meštrović, *J.Power Sources*, **196** (2011) 4849
18. B. Conway, Electrochemical Supercapacitors – Scientific Fundamentals and Technological Applications, Plenum Publishers, New York, USA, 1999
19. W. H. Mulder, J. H. Sluytes, T. Pajkossy, I. Nyikos, *J. Electroanal. Chem.*, **285** (1990) 103
20. D. Sačer, M. Kralj, S. Sopčić, M. Košević, A. Dekanski, M. Kraljić Roković, *J. Serb. Chem. Soc.*, **82** (2017) 411
21. V. V. Panić, A. B. Dekanski, R. M. Stevanović, *J. Power Sources*, **195** (2010) 3969
22. V. V. Panić, T. R. Vidaković, A. B. Dekanski, V. B. Mišković-Stanković, B.Ž. Nikolić, *J. Electroanal. Chem.*, **609** (1990) 120
23. C. Criado, P. Galán-Montenegro, P. Velásquez, J. R. Ramos-Barrado, *J. Electroanal. Chem.*, **488** (1990) 59